

THE USE OF ISENTROPIC ANALYSIS IN  
DEDUCING OCEANIC FLOW PATTERNS  
IN A REGION OF UPWELLING

—♦♦♦—  
H. R. SEAY

THESIS  
5400

Library  
U. S. Naval Postgraduate School  
Monterey, California





Mont  
56



THE USE OF ISENTROPIC ANALYSIS IN DEDUCING  
OCEANIC FLOW PATTERNS IN A REGION OF UPWELLING

H. R. Seay





THE USE OF ISENTROPIC ANALYSIS IN DEDUCING  
OCEANIC FLOW PATTERNS IN A REGION OF UPWELLING

by  
Howard Rodwell Seay  
Lieutenant, United States Navy

Submitted in partial fulfillment  
of the requirements  
for the degree of

MASTER OF SCIENCE  
IN AERONAUTICS

United States Naval Postgraduate School  
Monterey, California  
1953



This work is accepted as fulfilling  
the thesis requirements for the degree of

MASTER OF SCIENCE  
IN AERONAUTICS

from the  
United States Naval Postgraduate School



## PREFACE

This paper presents the results of isentropic analysis in depicting oceanic flow patterns in a region of known upwelling.

Undertaken as a requirement for the degree of Master of Science in Aerology, this investigation was conducted at the U. S. Naval Postgraduate School, Monterey, California during the period from August 1952 to January 1953.

Grateful acknowledgment is made for the advice and assistance rendered by Assistant Professor Jacob B. Wickham in the preparation of this paper.



## TABLE OF CONTENTS

	Page
CERTIFICATE OF APPROVAL	i
PREFACE	ii
TABLE OF CONTENTS	iii
LIST OF ILLUSTRATIONS	iv
TABLE OF SYMBOLS AND ABBREVIATIONS	v
CHAPTER	
I. INTRODUCTION	1
II. DATA USED IN INVESTIGATION	6
III. METHOD OF ANALYSIS	8
IV. INTERPRETATION OF RESULTS AND CONCLUSIONS	10
BIBLIOGRAPHY	18





# LIST OF ILLUSTRATIONS

Page

Figure 1	Vertical displacement of selected $\sigma_t$ surfaces from February to March, 1950, for Station Line 80	11
Figure 2	Vertical temperature sounding at Station 83-60 for July 1950, with indicated depth of the $\sigma_t = 26.00$ surface	14

## PLATE

(inside back cover)

I	Geographic area investigated with position of oceanographic station used in investigation
II	Plot of computed wind components parallel to the coast against time for period 1 February to 31 July 1950. Shaded areas represent time involved in completing oceanographic observations during each month.
III-XVII	Monthly salinity distributions on selected $\sigma_t$ surfaces. Isohalines are constructed for every .05 o/00. The whole numbers 33 and 34 have been omitted in labeling isohalines. Included on each chart is the bathymetric topography of the given surface. Isobaths are constructed for each 25 meters. Current arrows depicting the major flow patterns as inferred from the salinity distributions are also included on each chart.



# LIST OF SYMBOLS AND ABBREVIATIONS

$D$	Depth
$\Delta D$	Geopotential height anomaly
$\delta$	Specific volume anomaly
$K$	Constant
$O_2$	Dissolved oxygen concentration
$PO_4-P$	Dissolved phosphate concentration
$\phi$	Latitude
$\rho$	Density
$\rho_t$	Density of sea water at $T$ and $S$ in situ and atmospheric pressure
$\rho_\theta$	Potential density
$S$	Salinity in grams of salt per kilogram of sea water
$T$	Mass transport
$T$	Temperature in degrees centigrade
$t$	Time
$\tau_a$	Wind stress
$u$	x component of motion
$v$	Wind velocity
$v$	y component of motion
$w$	z component of motion



## I. INTRODUCTION

The phenomenon of upwelling, present wherever surface divergence exists, is of special interest in coastal regions. It is of profound commercial importance locally, as it pertains to the life cycle of the California sardine. Indeed the commercial importance of the sardine led to the organization of California Cooperative Sardine Research Program to investigate the virtual disappearance of the species from commercially accessible fishing grounds. The oceanographic observations collected in the routine operations of this program form the data basis for this paper. Aside from the commercial aspects of the upwelling process, it is of importance to naval operations in ocean areas. Successful submarine detection depends, to a large degree, upon the vertical temperature distribution in the sea which is profoundly effected by the process of upwelling.

A qualitative explanation of the process based upon Ekman's theory of wind driven currents was first suggested by Thorade [9] in 1909 and later developed by McEwen [1] in 1912. Ekman's theory, in part, states that the mass transport caused by wind stress upon the sea surface is directed at right angles ~~cum~~ <sup>cross</sup> to the wind direction. The wind acts to the depth of effective frictional resistance. Ekman [8, p 494] derived the empirical relation  $D = 7.6 \frac{V}{15 \sin \phi}$  for this depth. It can be seen from this equation that the depth to which the influence of the wind is felt depends upon latitude and wind speed. The mass transport as given by  $T = K \frac{\tau_a}{\rho}$  [8, p 498] is a function of latitude and  $\tau_a$ .





$\tau_a$  in turn is a function of  $v^2$  as can be seen by the expression for stress  $\tau_a = 2.6 \cdot 10^{-3} \rho v^2$  [8, p 490] where  $v$  is the wind at 15 meters above the surface.

Consider a coast in the northern hemisphere with a wind blowing parallel to the coast such that the coast lies to the left of the wind. The mass transport of the wind driven current will be confined to the levels above  $D$  and will be directed away from the coast, thus the surface waters will be transported off shore at a rate proportional to the square of the wind speed. The continuity of the system requires that sub-surface waters rise to replace this mass deficiency. During the spring and summer months the semi-permanent Pacific anticyclone is established providing fairly steady winds roughly parallel to the central and southern California coasts, and it is during this period that upwelling becomes a conspicuous feature.

The phenomenon has been widely examined since the qualitative explanation was developed. Special aspects of the problem have received attention with emphasis upon the velocity of the vertical motion [2] and the depth from which water is brought to the surface [7]. A more detailed investigation of the phenomenon was undertaken by Sverdrup [6] in 1938 using a single station line at right angles to the California coast off Port San Luis. From three series of observations taken in March, May and July of 1937 along this station line, Sverdrup was able to develop a vertical section depicting the circulation perpendicular to the coast. The measured vertical motion of substantial surfaces coupled with the principals of the equation of





of continuity to obtain horizontal components of motion was the analysis tool. This investigation, however, was based upon limited data and assumed uniform velocity parallel to the coast. McDwen [3] has investigated the horizontal circulation associated with large scale horizontal eddys forming in conjunction with the upwelling process using the dynamic concept of the conservation of angular momentum. However, no investigation of the regions of upwelling have, to the author's knowledge, been made upon the basis of isentropic analysis.

The validity of flow patterns inferred from isentropic analysis has been discussed by Parr [5] and Montgomery [4]. A general review of the concepts of isentropic analysis seems appropriate before proceeding further. As is well known, surfaces in the atmosphere defined by constant potential temperature are surfaces along which adiabatic interchange of air masses, assuming air to be a perfect gas, result in no change in the distribution of mass. These surfaces are then isentropic surfaces. The question arises, are there surfaces in the sea which are isentropic.

Montgomery [4] states that

there exists no patent mechanism for altering the potential density of any water particle below the layer of direct surface influence. Therefore no flow of major proportions can take place across surfaces of constant potential density.

Actually, as demonstrated by Sverdrup [8, p 417], there exist no true isentropic surfaces in the sea; however, potential density surfaces are quasi-isentropic, implying that along these surfaces interchange of water masses result in only small changes in the mass



distribution. It is possible to determine potential density surfaces in the sea. However, the normal density parameter observed in oceanographic work is  $\sigma_t$ , where  $\sigma_t$  is defined as  $(\rho_t - 1) 1000$ .  $\rho_t$  is the density at temperatures and salinities in situ but at atmospheric pressure. The difference between  $\rho_t$  and  $\rho_0$ , the potential density, is negligible above 1000 meters. This is demonstrated by Montgomery [4], who shows that the adiabatic temperature changes involved in bringing a water particle from depths less than 1000 meters to the surface are small. Thus it is permissible to use  $\sigma_t$  surfaces as quasi-isentropic surfaces in water of depths less than 1000 meters.

As in atmospheric isentropic analysis, the distribution of a conservative property on the surface is employed in making inferences as to the flow pattern. Moisture concentrations, as shown by specific humidity, are used as the conservative property in the atmosphere; in the ocean salinity is the conservative property used. If a maximum of the conservative property is found on the isentropic surface, it will, under the influence of a current on the surface, move with the current. As it moves, isentropic mixing along the surface will tend to reduce the intensity of the maximum in the direction of the current. If, at the same time, high concentrations are maintained at the original point of the maximum by some other process, then a tongue of maximum, but decreasing, concentration indicates a current along the tongue axis with flow toward low concentrations. Although there are no true isentropic surfaces in the oceans, lateral mixing along  $\sigma_t$  surfaces is quasi-isentropic.





Waters of differing salinities mixing along these surfaces will retain, approximately, their original densities; i.e., the products of mixing will remain upon the surface.

Consider a concentration of high salinity water upon a  $\sigma_t$  surface, with a source of high salinity water to maintain the maximum. If a current on the surface moves through the area of maximum salinity, a tongue of high salinity will extend in the direction of current flow in a manner similar to the situation shown in atmospheric isentropic analysis. Thus flow patterns can be inferred from the distribution of high or low salinity tongues on  $\sigma_t$  surfaces. This is, of course, a generalization of Wüst's Kernschicht method of tracing absolute salinity maximums in the vertical, as shown by Montgomery [4].

It is apparent from this discussion that isentropic analysis as applied to the oceans is primarily qualitative rather than quantitative. The descriptive nature of such analysis is, of course, an end in itself and can provide valuable information without the knowledge of actual current velocities. Possible quantitative results will be discussed in a later chapter.

The use of salinity as a conservative property may be questioned on the grounds that density is not independent of salinity; however, density does not depend entirely upon salinity. If there existed a unique relationship between density and salinity then salinity surfaces and density surfaces in the ocean would be parallel. However, these surfaces do intersect, so it would seem that the distribution of salinity upon a  $\sigma_t$  surface is brought about by the flow patterns and the mixing which exist.



## II. DATA USED IN INVESTIGATION

The data used in this investigation were provided by the operations of the California Cooperative Sardine Research Program. The raw data has been processed and published by Scripps Institute of Oceanography. The area investigated is shown in Plate I which includes the positions and number designators of the oceanographic station used. These stations, in the course of the program, were occupied monthly by vessels of the Research Program and observations of the following parameters were made:

- (1)  $T$
- (2)  $S$
- (3)  $O_2$
- (4)  $PO_4-P$

The values of these were interpolated graphically to standard depths, and, from (1) and (2), values of the following parameters were determined for standard depths:

- (5)  $\sigma_t$
- (6)  $10^5 \delta$
- (7)  $\Delta D$

The parameters used in this investigation were:

- (1)  $D$
- (2)  $S$

It was necessary to assume that the data were synoptic in nature. Actually the time interval involved in completing the observations for the area under investigation varied from a minimum of 5 days in March,





when not all stations were occupied, to a maximum of thirteen days in May. Since conditions in the oceans change slowly, this assumption does not invalidate the resulting general features of the flow; but it does make any interpretation of the minor features doubtful.

It is also necessary to assume that station positions were fixed from month to month. This assumption is not quite fulfilled, but the error is small since the maximum deviation from one month to the next was two nautical miles. The error involved in this assumption is probably negligible compared to errors in the assumption of synopticity.

All parameters were assumed to vary linearly between standard depths. This assumption reduced the labor and time of interpolation considerably. Since the data as received was interpolated to standard depths, it was felt that little accuracy could be gained by vertical plots of the parameters in an attempt to reproduce the original sounding. In view of the above, and because the results are intended to be qualitative, the time saving computational method of interpolation was felt to be justified.

The file of analyzed weather charts of North America and Pacific ocean areas maintained by the Naval Postgraduate School, Monterey, California, were utilized to determine wind components parallel to the coast during the period investigated. The calculated values of the wind component are qualitative in nature. This is true because the area concerned represents a small segment of the analyzed weather chart and, in many cases, isobaric spacing could be adjusted through wide ranges, while still satisfying the surface reports. In all cases possible, results of geostrophic measurements were checked against observed winds to reduce errors.



### III. METHOD OF ANALYSIS

As a first step, the component parallel to the coast of the average wind over the area was computed in this matter. The average geostrophic wind over the area was measured directly from the daily 1230 GCT analyzed chart for the period from 1 February to 31 July. The winds were assumed to deviate ten degrees from the isobars, and corrections for isobaric curvature and air mass stability were made in accordance with the procedure outlined in H. O. 604 [10, pp 16-17] . An average stability factor of .60 was selected for the entire period. This represents a sea temperature minus air temperature difference of from one to seven degrees. The components of these winds parallel to the coast were computed and five day means of these values were plotted. The results are shown in Plate II. The hatched areas in the figure represent the time interval involved in the cruises during each month. Since the stress exerted by the wind upon the sea surface is a function of the square of the wind speed, it would seem appropriate to graph these values rather than the actual wind speeds, but in this investigation only the qualitative aspects of the wind in producing upwelling is necessary.

Inspection of the diagram shows considerable variability in the coastal components, but several features are immediately apparent. The winds conducive to upwelling begin early in February and continue throughout the period. The period between May and June show the weakest and most erratic values, while the eighteen day periods prior to the May and July oceanographic observations show relatively steady components of moderate velocities following periods of maximum velocities. From this





it is inferred that the beginnings of the upwelling should be apparent in March and that the maximum upwelling should be apparent in May and July.

The second step in the investigation was the preparation of isentropic charts for the months of February through July. The surfaces  $\sigma_t = 26.00$  and  $\sigma_t = 26.50$  were selected except for the month July, in which month the additional surfaces  $\sigma_t = 26.75$  ,  $\sigma_t = 27.00$  and  $\sigma_t = 27.25$  were also investigated. This additional analysis was undertaken in order to obtain a more detailed picture in July which, on the basis of the  $\sigma_t = 26.00$  and  $\sigma_t = 26.50$  surfaces, appeared to be the month of most pronounced upwelling (see Chapter IV). The distribution of salinity on these selected surfaces was determined by linear interpolation from values at standard depths. Also the geometric depths of the selected surfaces were similarly determined. These two values, salinity on the surface and the depth of the surface, were determined for each station for each month. Isohalines were then drawn on each surface; and, on the same chart, the bathymetric topography of the given surface was also drawn. The results are shown in Plates III-XVII.

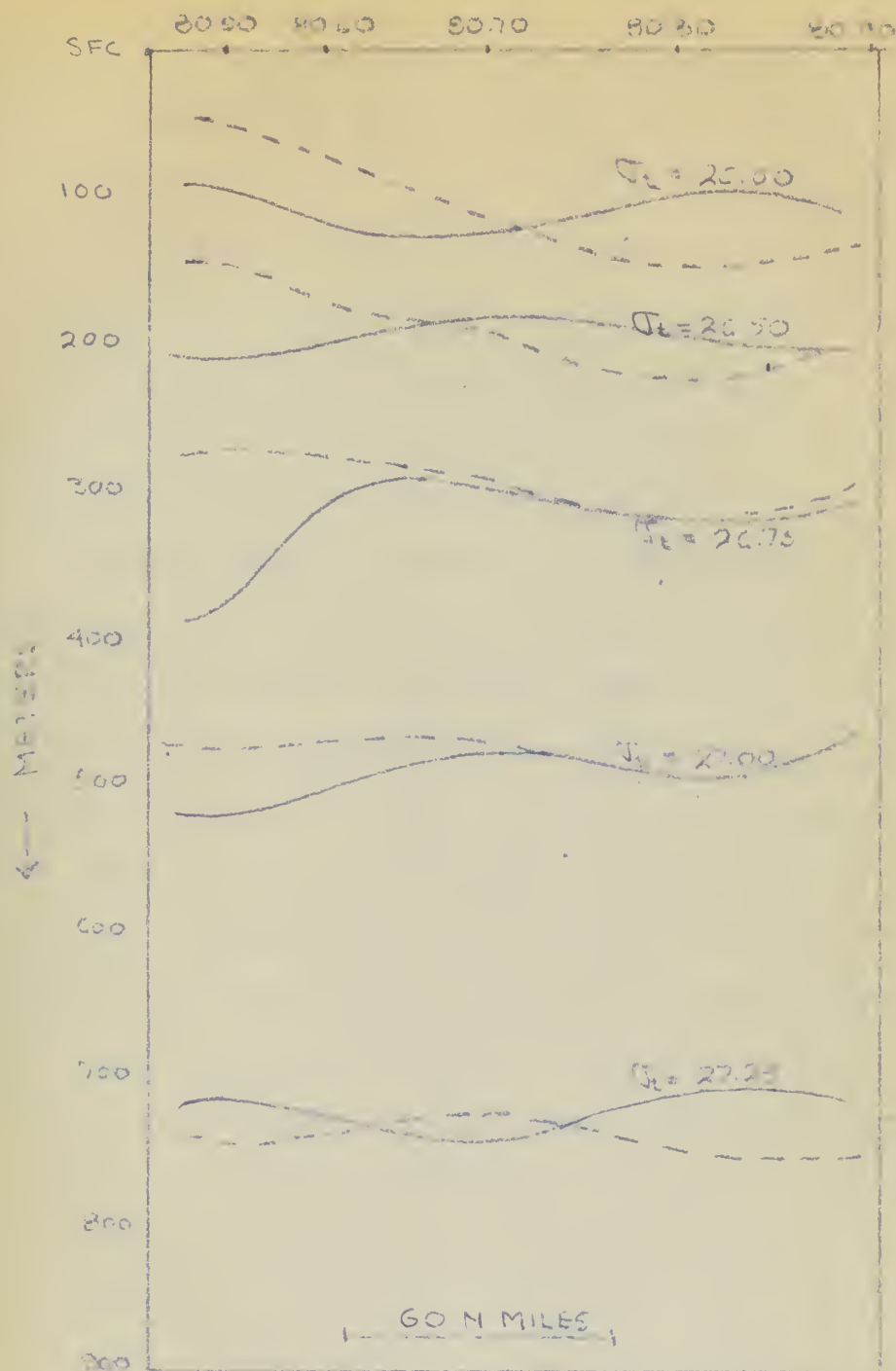


#### IV. INTERPRETATION OF RESULTS AND CONCLUSIONS

As discussed in Chapter I, salinity distributions on  $\sigma_t$  surfaces are assumed to indicate flow patterns. In accordance with this, arrows depicting the general flow pattern have been constructed on the basic charts (Plates III-XVII). Inspection of the charts shows two prominent features. First, a large cyclonic eddy is evident on all charts except the  $\sigma_t = 27.25$  surface for July, where the pattern breaks down at these great depths. This eddy's presence is inferred from the tongue of low salinity which extends toward the coast in the southern portion of the area and then curves northward inshore. Second, the isolated maximums of salinity occur on domes in the  $\sigma_t$  surfaces, while conversely isolated minimums occur on depressions in the surfaces. The first feature is not surprising since the shoreward extension of low salinity water and the existence of the large cyclonic eddy have been demonstrated by other methods in previous investigations of the same general area [11, p 27]. This feature then, as depicted by isentropic analysis, substantiates other findings. The second feature is of more interest to the author. Under the assumption that  $\sigma_t$  surfaces are substantial surfaces it follows that, if vertical motion occurs within a region, the surfaces must move with the water. It will be recalled that, on the basis of the longshore wind component calculations (see Plate II), March was the month during which upwelling should first occur. Figure 1 demonstrates the effect of the upwelling upon the  $\sigma_t$  surfaces during the interval between February and March. The vertical section shown in Figure 1 is for station line 80. Upward motion is indicated inshore of station 80-70







Vertical section through Station Line 80 showing  
vertical displacement of selected  $\sigma_t$  surfaces  
from February to March 1950  
 — February surfaces  
 --- March surfaces  
 Depth in meters

Figure 1



to depths of at least 500 meters, while downward motion is shown west of station 80-70 to depths below 200 meters. This downward motion is to be expected west of the area of strongest longshore wind components since the decreasing wind stress would produce decreasing offshore transport and surface convergence would occur, necessitating motion downward. The decreasing wind velocity and, thus, wind stress is to be expected since the pressure gradient in the high pressure cell giving rise to the winds decreases toward the center of the high.

The average upward displacement of the  $\sigma_t$  surfaces in the inshore area is approximately 40 meters, and a simple calculation gives the average vertical velocity, based upon the  $\sigma_t$  surface displacements, as  $1.5 \times 10^{-3}$  cm/sec. If the surface divergence responsible for this upwelling continues, motion must take place through the  $\sigma_t$  surfaces because these surfaces seem to become stationary near, but below, the sea surface. This means that, in the region of continuing surface divergence, the compensating inflow from below cannot be isentropic, since, by definition, any component of motion which crosses the  $\sigma_t$  surfaces is non-isentropic. If the component of the wind parallel to the coast can be used as an indicator of surface divergence, then surface divergence was a continuous phenomenon throughout the period under investigation. Inspection of the data for this period shows that salinity increases with depth at any given station except for minor variations. This means that no major salinity maximums or minimums exist in the vertical. This observation offers a clue to the origin of the salinity maximums and minimums appearing on the  $\sigma_t$  surfaces,

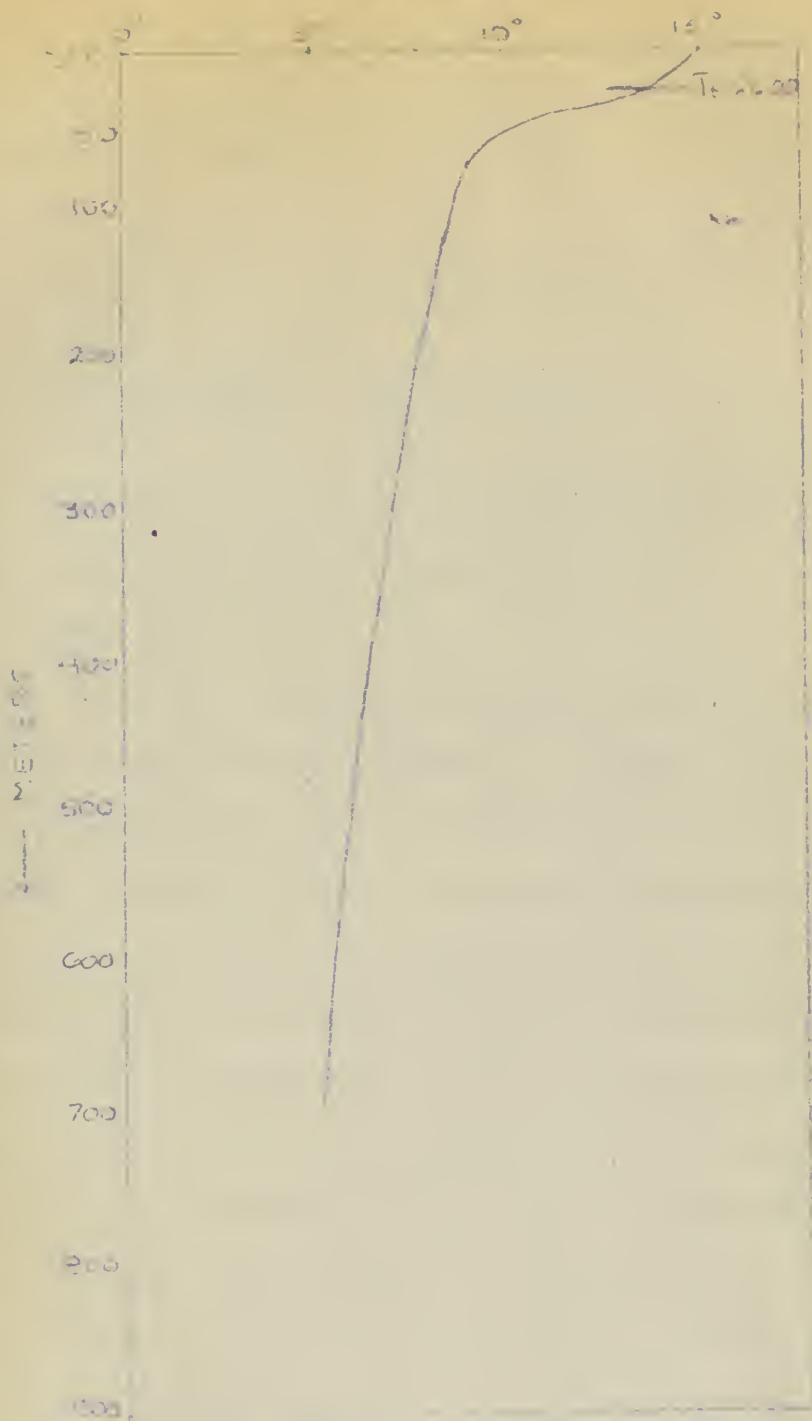


namely, that water characterized by high salinity on a given  $\sigma_t$  surface comes from depths below the level of that surface. Conversely, low salinity water on a given surface comes from depths above the level of that surface. If the above reasoning is valid, then salinity extremes on a given  $\sigma_t$  surface indicate vertical mixing, which is non-isentropic, or some other non-isentropic process.

Montgomery [4] has discussed a non-isentropic process to allow for the upwelling necessary to compensate for surface divergence. This process he calls mixing upward and concludes that it is due to vertical turbulence occurring at the boundary of the homogenous layer. He further concludes that this vertical mixing cannot extend deeper than the lower boundary of the layer of surface influence (see Chapter I). Assuming that mixing upward will compensate for the surface divergence, it becomes necessary to explain the formation of the salinity maximum on the elevated  $\sigma_t$  surfaces near the lower boundary of the layer of surface influence. An example of this situation is shown on Plate XIII where the  $\sigma_t = 26.00$  surface lies between 50 and 75 meters in the region southwest of the Channel Islands with the associated salinity maximum on the  $\sigma_t$  surface. A vertical temperature sounding for Station 83-60 which lies in the region of the elevated  $\sigma_t$  surface, is shown in Figure 2 with the depth of the  $\sigma_t = 26.00$  surface indicated on the sounding. The figure shows that the  $\sigma_t = 26.00$  surface lies at the lower boundary of the layer of surface influence. Consider a point on this boundary; if water from below is to penetrate to levels above this boundary, then the density of this penetrating water must be altered by some non-isentropic process. If this







Vertical temperature sounding Station 83.60  
 July 1950. Depth of  $\sigma_t = 26.00$  surface indicated  
 Depth in meters  
 Temperature in degrees  
 Centigrade

Figure 2





were not true the  $\sigma_t = 26.00$  surface would move upward and penetrate to the surface, and this is not observed. According to the observation, the local rate of change of density,  $\frac{\partial \rho}{\partial t}$ , at the lower boundary of the surface layer must equal 0. The rate of change of density of a moving particle may be expressed as the sum of the local and advective rates of change of density:

$$\frac{d\rho}{dt} = \frac{\partial \rho}{\partial t} + \frac{\partial \rho}{\partial x} u + \frac{\partial \rho}{\partial y} v + \frac{\partial \rho}{\partial z} w$$

Assuming horizontal advection to be small in the region of maximum upward mixing, this expression reduces to

$$\frac{d\rho}{dt} = \frac{\partial \rho}{\partial z} w$$

The individual rate of change of density is, under these assumptions, equal to the vertical advection of density. A possible explanation for the decrease in density of the water particle as it moves into the surface layer is by eddy diffusion of heat from the warmer surface layer. This eddy diffusion, or mixing, does not appreciably decrease the salinity, however, as salinity gradients in the mixed layer are very small. The heat content of this layer is replenished, in turn, by solar radiation. Thus the density of the particle could be decreased without appreciably decreasing the salinity, resulting in a concentration of high salinity water appearing on the elevated  $\sigma_t$  surface immediately below the surface layer. It is interesting to note that calculations, not presented here, using the concept of density decrease by solar radiation give a vertical velocity, of the upward moving particle, of the same order



of magnitude as the vertical velocities of upward motion deduced from the vertical displacement of the  $\sigma_t$  surfaces early in the upwelling period.

The salinity maximums evident upon the  $\sigma_t = 26.00$  surfaces, when they are close to the sea surface in other months, can be explained by the same reasoning, if this reasoning is valid.

The existence of salinity minimums on the deeper  $\sigma_t$  surfaces and the existence of both maximums and minimums at intermediate depths, which are particularly evident on the  $\sigma_t = 26.75$  and  $\sigma_t = 27.00$  surfaces for July (see Plates XV and XVI), are probably due to vertical mixing, but the cause of such mixing is not readily apparent. Internal waves, characterized by large velocity shear across interfaces, are a possible general explanation of pronounced vertical mixing at depths where salinity maximums and minimums appear. Another factor to be considered is the effect of bottom friction in producing turbulent vertical mixing. However, it is beyond the scope of this investigation to assess the influence of these factors upon the observed salinity distributions.

As discussed in Chapter I, the concept of upwelling associated with wind driven currents requires a transport of water perpendicular to the wind direction. In the area under investigation, this transport is, of course, directed offshore. Evidence of this offshore transport is inferred from the salinity distribution on the  $\sigma_t = 26.00$  surface for May (Plate IX) and the  $\sigma_t = 26.00$  surface for July (Plate XIII). The pronounced high salinity tongue extending offshore from the salinity



maximums in the region south of the Channel Islands is, in each case, considered to give evidence of this offshore transport. As discussed in Chapter III, the results of the longshore wind component computations indicated that May and July should be the months of maximum upwelling, and the observed salinity distribution on the upper  $\sigma_t$  surface indicates that the offshore transport was most pronounced during these months.

Longshore transport of the more saline upwelled water is inferred from the southward extension of high salinity tongues on the  $\sigma_t = 26.00$ , 26.50, 26.75 and 27.00 surfaces for July (Plates XIII-XVI). This result is in qualitative agreement with previous investigations of the area [11, p 27] which indicate that the more saline waters are carried south from the region of upwelling by the eastern edge of the California current.

The results of this investigation have verified, in the author's opinion, results previously obtained by different methods; and, as such, have proved of some value. More investigation of the processes giving rise to the observed salinity maximums and minimums on  $\sigma_t$  surfaces is necessary before these distributions can be said to be of significance in picturing the centers of upwelling or subsidence. The qualitative nature of isentropic analysis can be overcome to some extent by considerations of diffusion and advection as effecting the distributions of some conservative property, e.g., salinity. Such calculations were beyond the scope of this investigation.





## BIBLIOGRAPHY

1. McEwen, G. F., The distribution of ocean temperatures along the West coast of North America deduced from Ekman's theory of the upwelling of cold water from adjacent ocean depths. Int. Revue d. gesamten Hydrobiol. U. Hydrogr., 1912
2. McEwen, G. F., Rate of upwelling in the region of San Diego computed from serial temperatures. Fifth Pac. Sci. Congress, 1933, Proc., Vol. 3, Univ. Toronto Press, 1933.
3. McEwen, G. F. Lecture notes. Scripps Institution of Oceanography.
4. Montgomery, R. B. Circulation in upper layers of Southern North Atlantic deduced with use of isentropic analysis. Papers in physical oceanography and meteorology. Vol. 6, No. 2. Cambridge, Mass. Mass. Inst. of Tech. Sept. 1938.
5. Parr, A. E., Isentropic analysis of current flow by means of identifying properties. Journal of Marine Research. 1:133-154. 1937-1938.
6. Sverdrup, H. U., On the process of upwelling. Journal of Marine Research. 1:155-164. 1937-1938.
7. Sverdrup, H. U., The origin of the deep-water of the Pacific as indicated by the oceanographic work of the "Carnegie". Intern. Geodet. Geophys. Union, Stockholm Assembly, Section of Oceanography, 1930.
8. Sverdrup, Johnson, and Fleming. The oceans. New York, Prentice-Hall, 1942.
9. Thorade, H., Uber die Kalifornischen, meeresstramungen, an der Westkuste Nordamerikas. An. d. Hydr. u. Met., Bd. 37., 1909.
10. U. S. Navy Hydrographic Office. H. O. Pub. No. 604., Techniques for forecasting wind waves, Washington, 1951.
11. State of California. Dept. of Fish and Game. California Cooperative Sardine Research Program, Progress Report. 1 Jan. 1951 to 30 June 1952. Sacramento, July 1952.

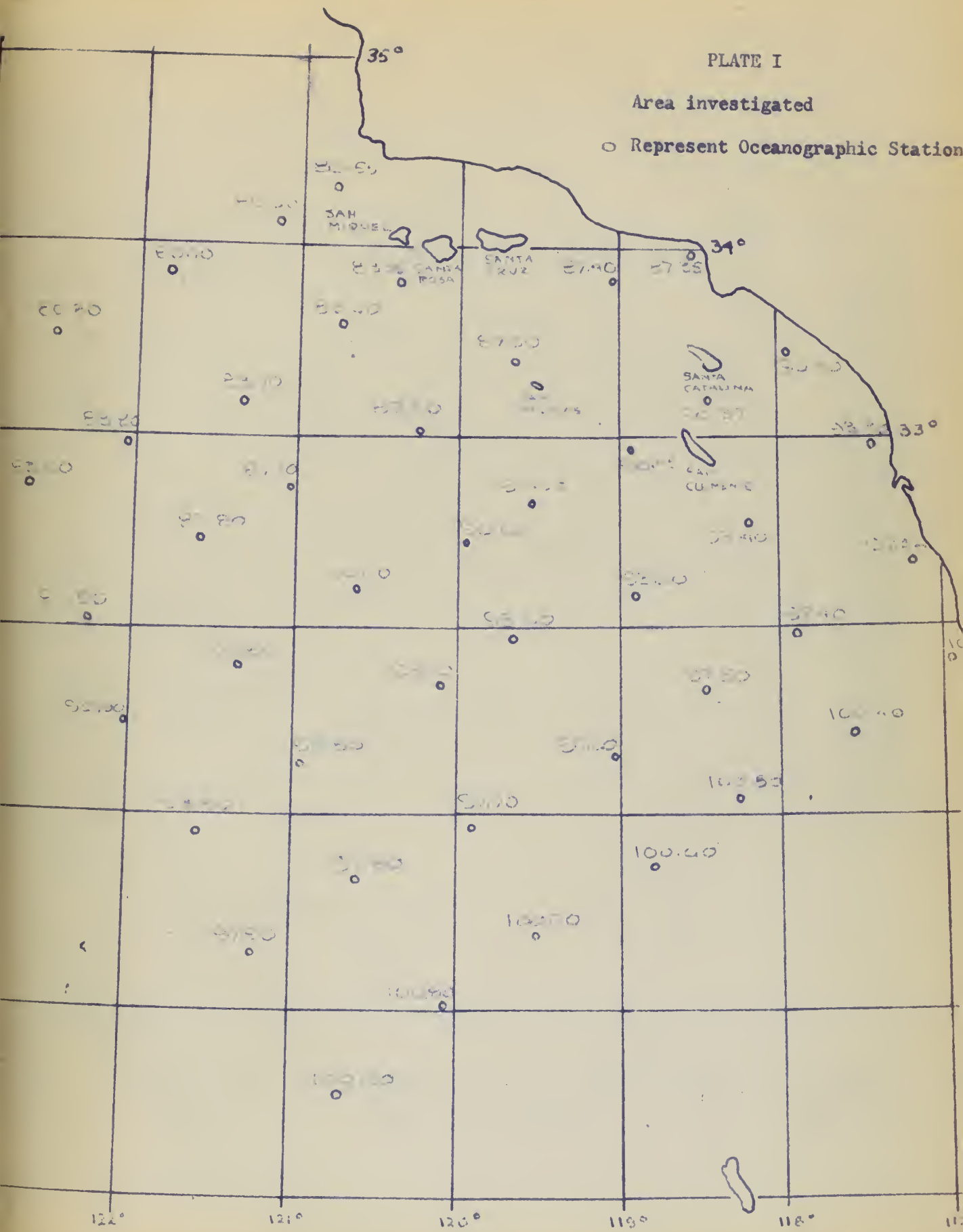




# PLATE I

Area investigated

○ Represent Oceanographic Station





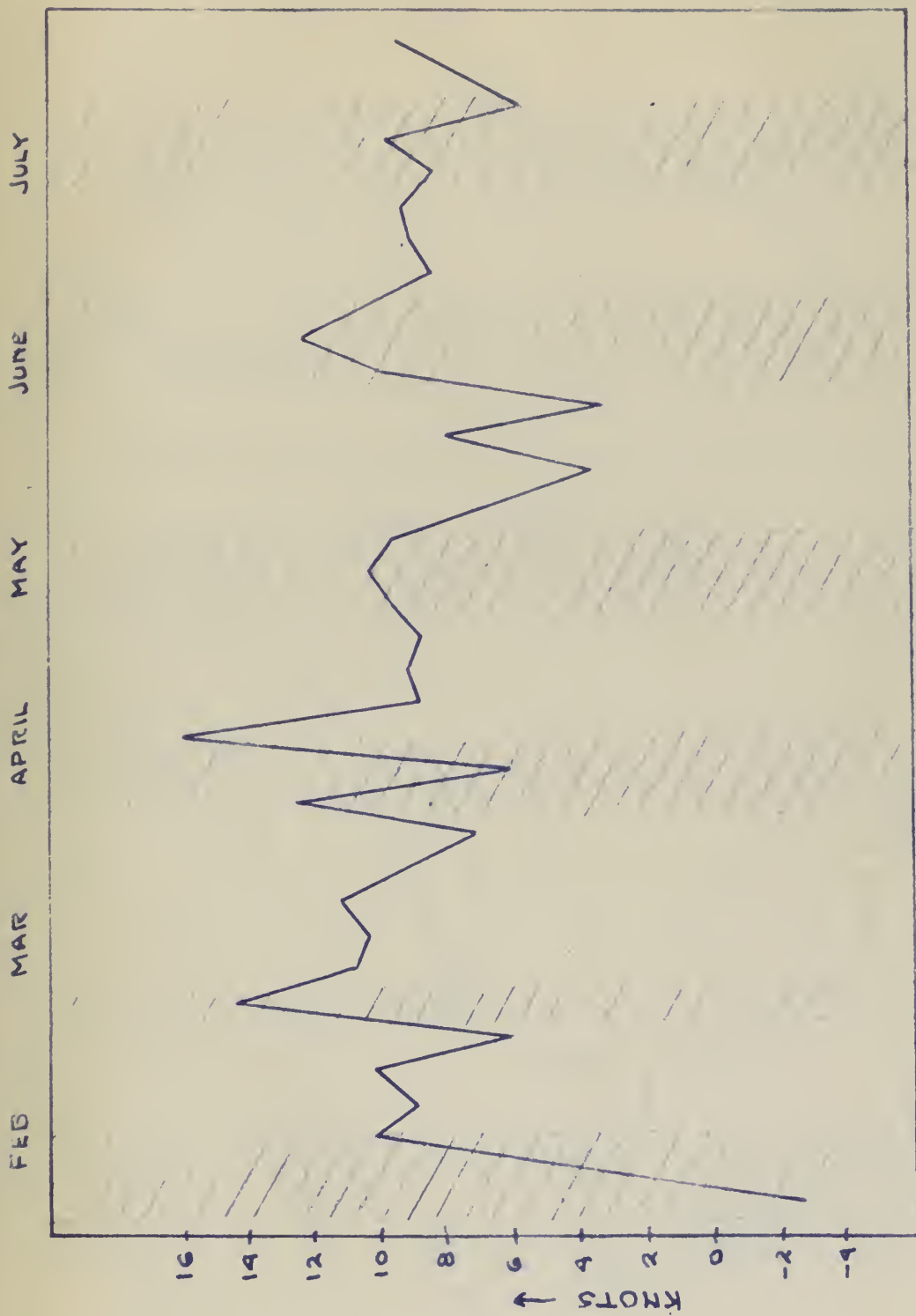


PLATE II

Plot of wind component parallel to coast, in knots.  
1 February to 31 July 1951. Shaded areas represent  
time involved in completing oceanographic observations.



PLATE III

Salinity distribution  
on  $\sigma_t = 26.00$  surface.  
February 1950

- - - 25 meter isobaths

— Salinity in o/00  
(whole numbers 33 and 34  
omitted from isohaline  
labels)

→ Inferred flow pattern

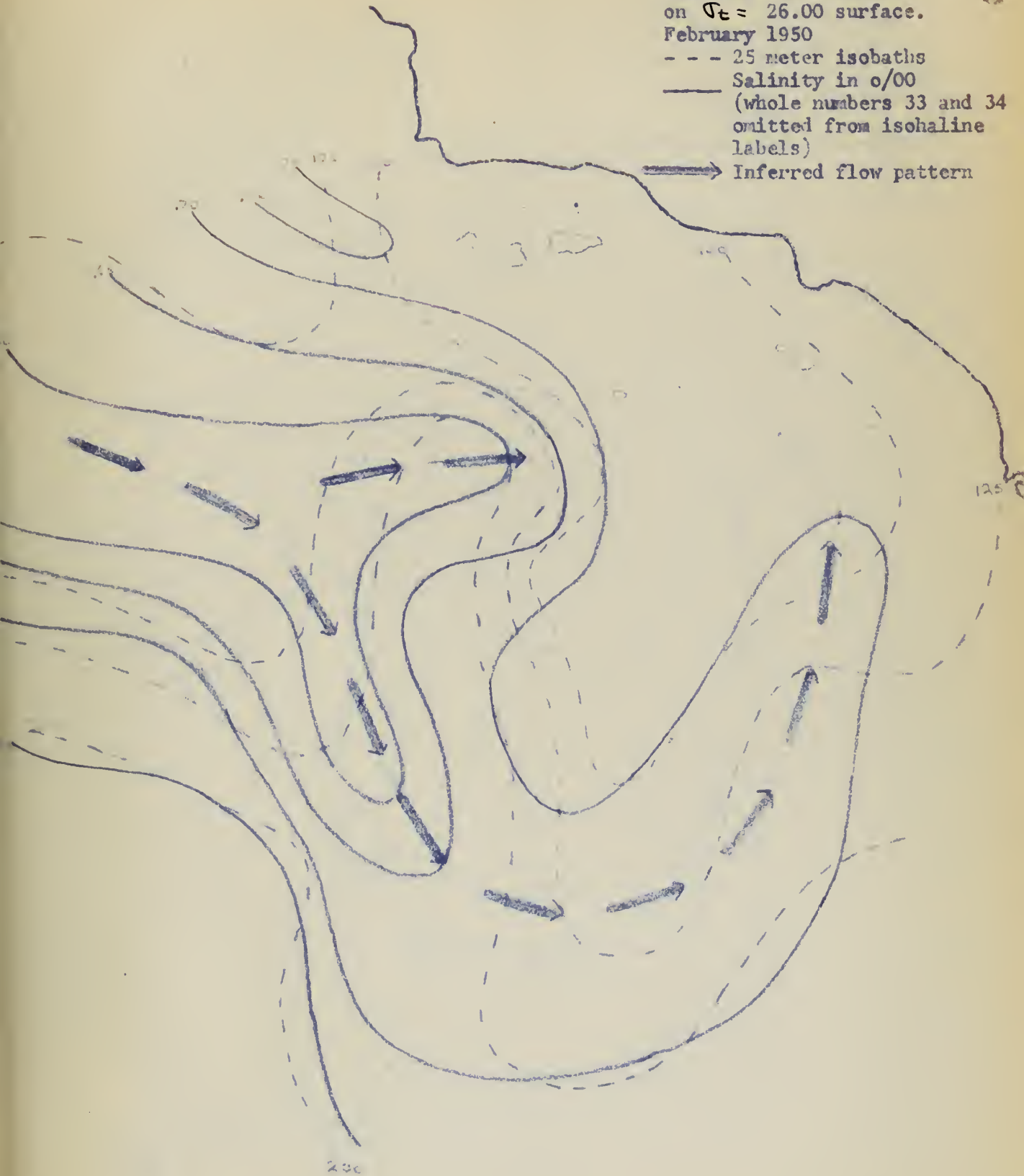






# PLATE IV

Salinity distribution  
on  $\sigma_t = 26.50$  surface  
February 1950

--- 25 meter isobaths

— Salinity in o/00  
(whole numbers 33 and 34  
omitted from isohaline  
labels)

➔ Inferred flow pattern

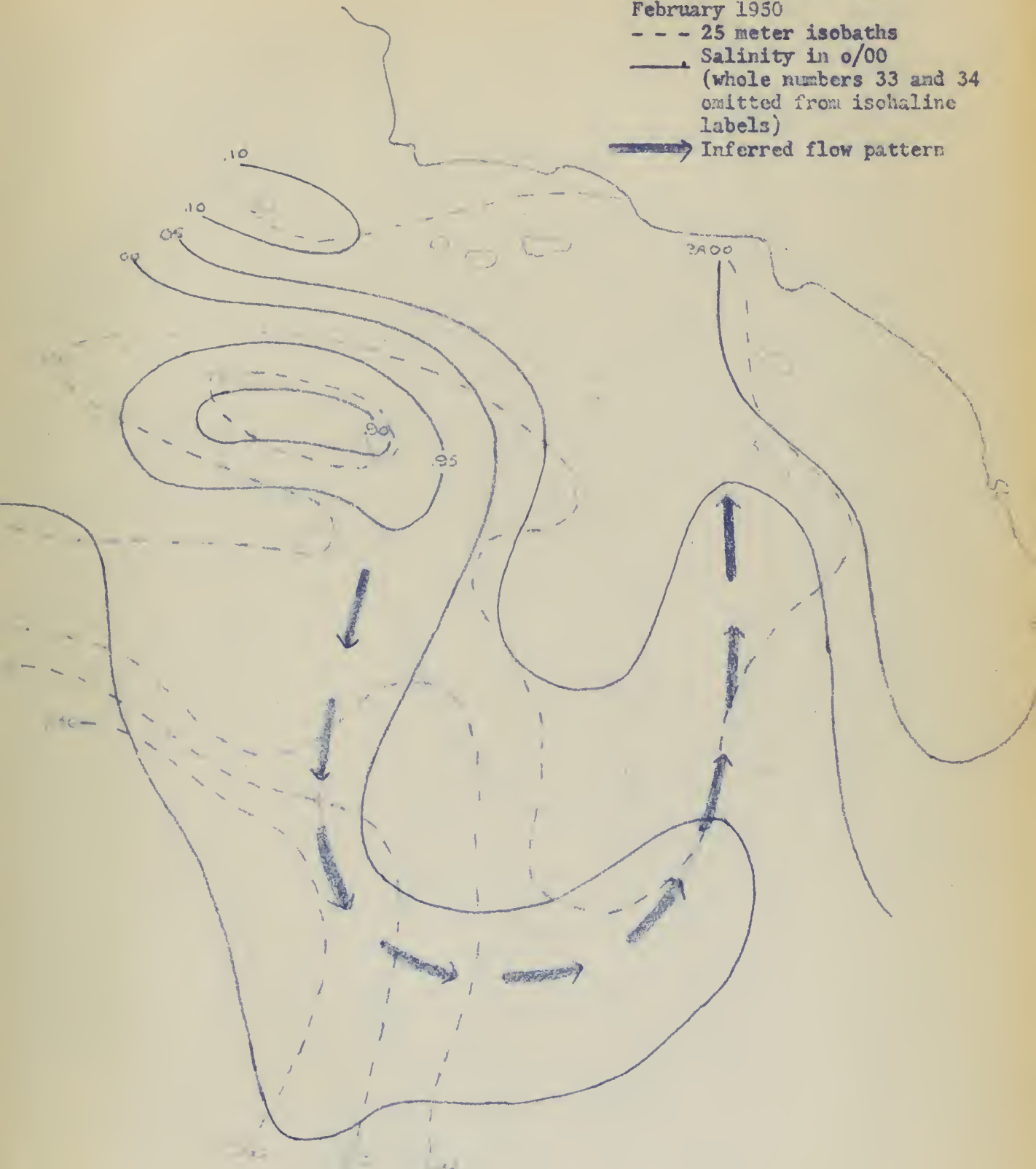




PLATE V

Salinity distribution  
on  $\sigma_t = 26.00$  surface  
March 1950  
- - - 25 meter isobaths  
—— Salinity in ‰  
(whole numbers 33 and 34  
omitted from isohaline  
labels)  
————→ Inferred flow pattern

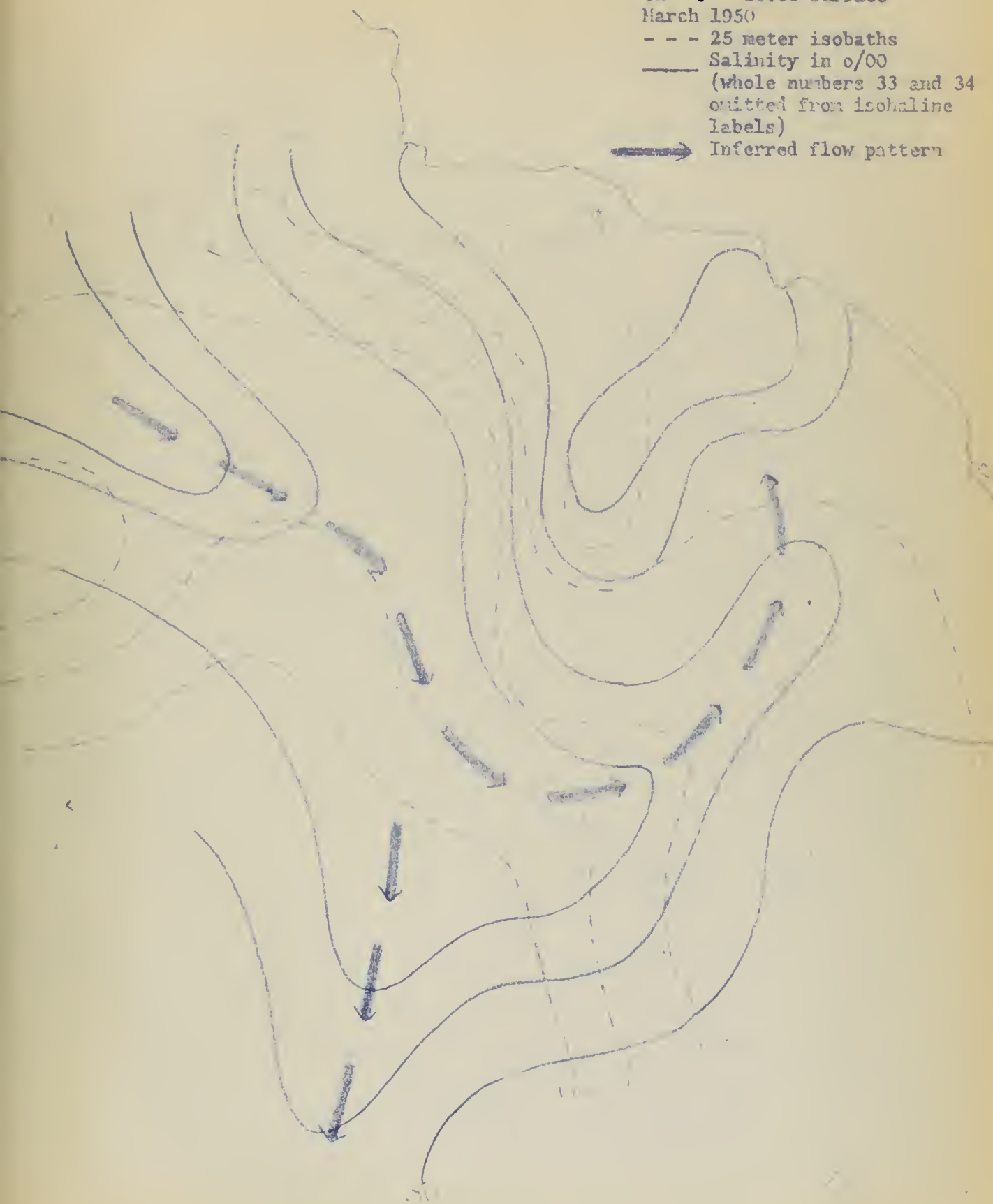




PLATE VI

Salinity distribution  
on  $\sigma_t = 26.50$  surface  
March 1950

- - - 25 meter isobaths

— Salinity in ‰  
(whole numbers 33 and 34  
omitted from isohaline  
labels)

→ Inferred flow pattern

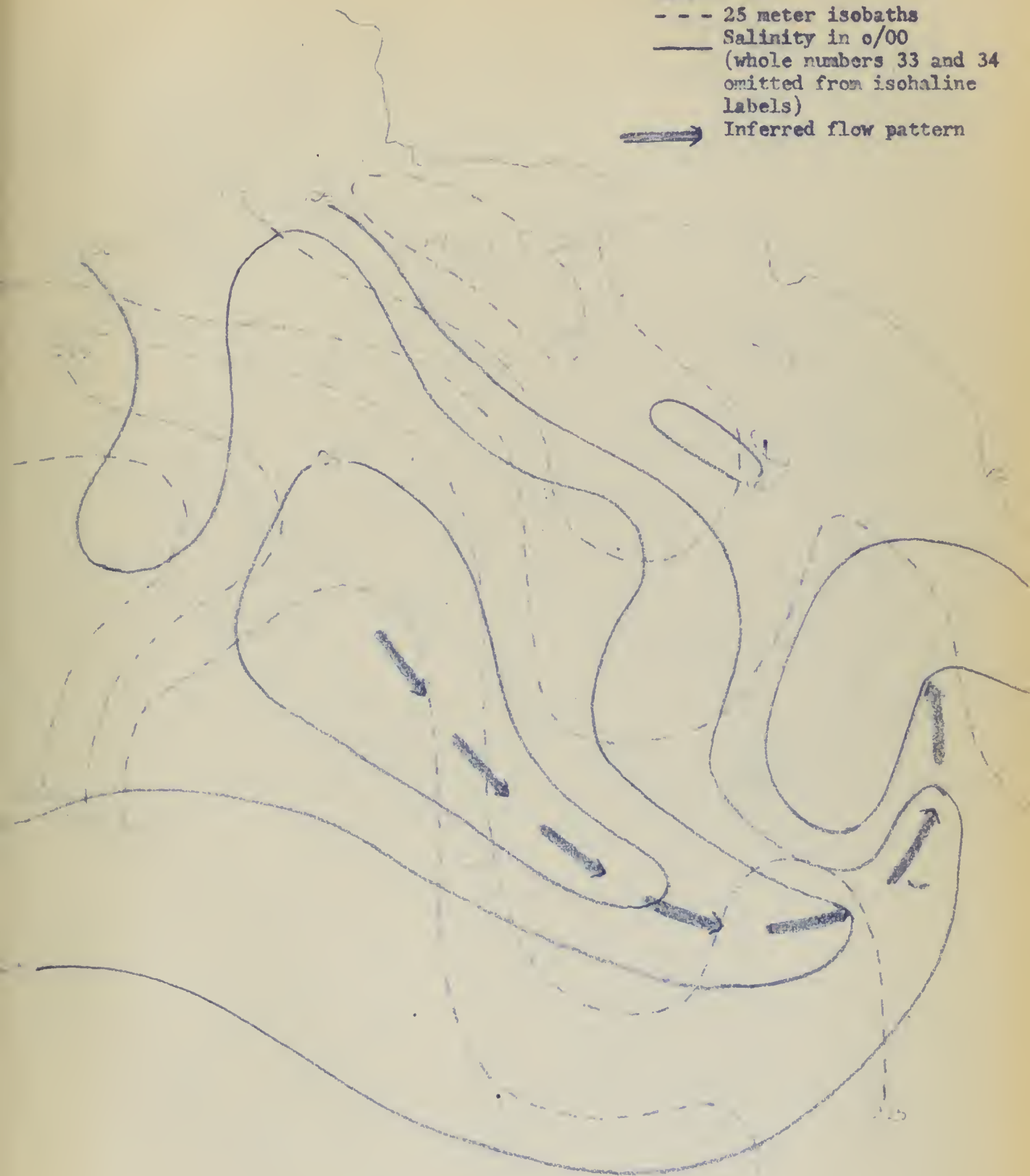




PLATE VII

Salinity distribution  
on  $\sigma_t = 26.00$  surface  
April 1950  
- - - 25 meter isobaths  
—— Salinity in o/00  
(whole numbers 33 and 34  
omitted from isohaline  
labels)  
➡ Inferred flow pattern

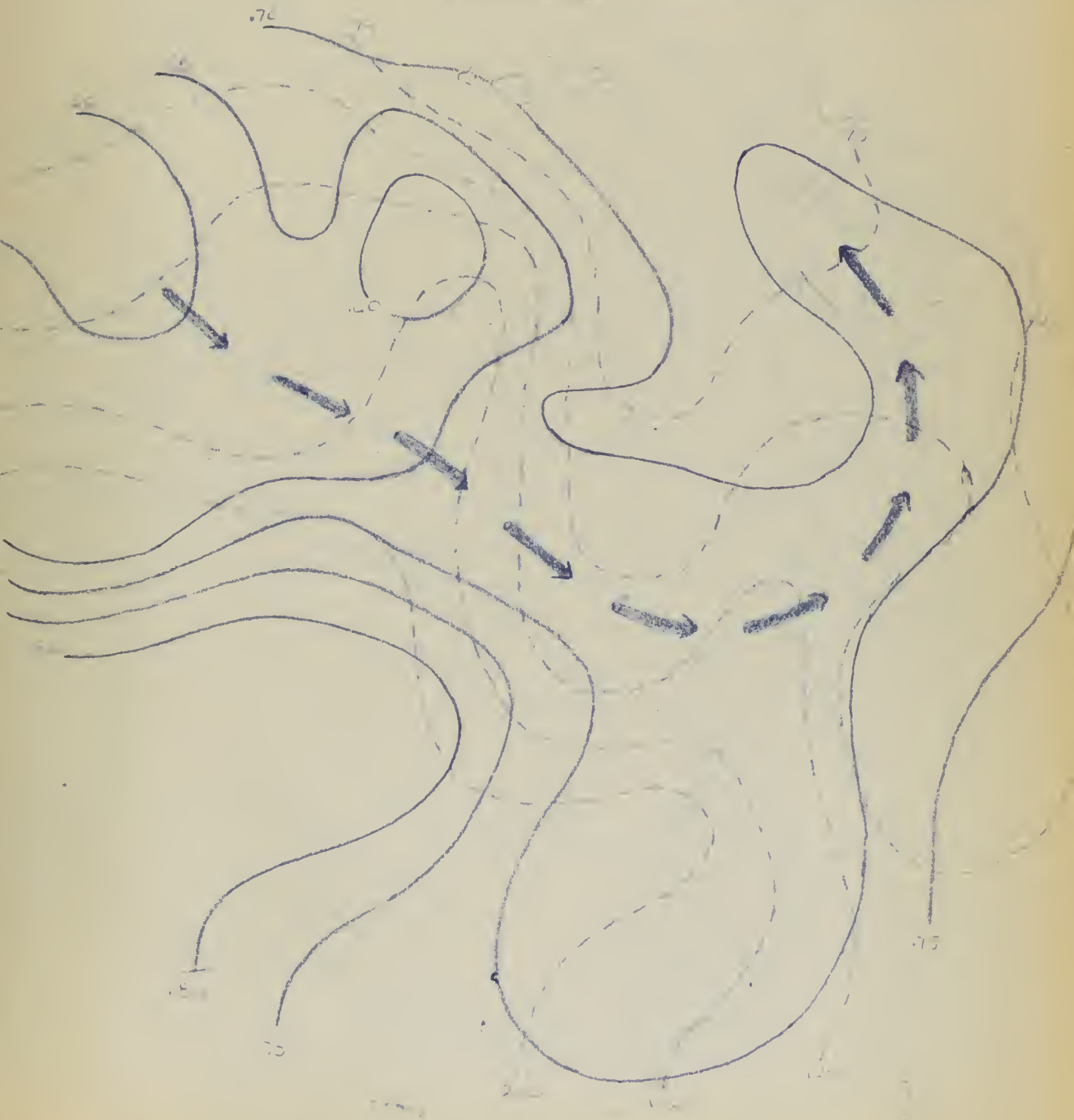






PLATE VIII

Salinity distribution  
on  $\sigma_t = 26.50$  surface  
April 1950

- - - 25 meter isobaths

— Salinity in o/00  
(whole numbers 33 and 34  
omitted from isohaline  
labels)

➡ Inferred flow pattern

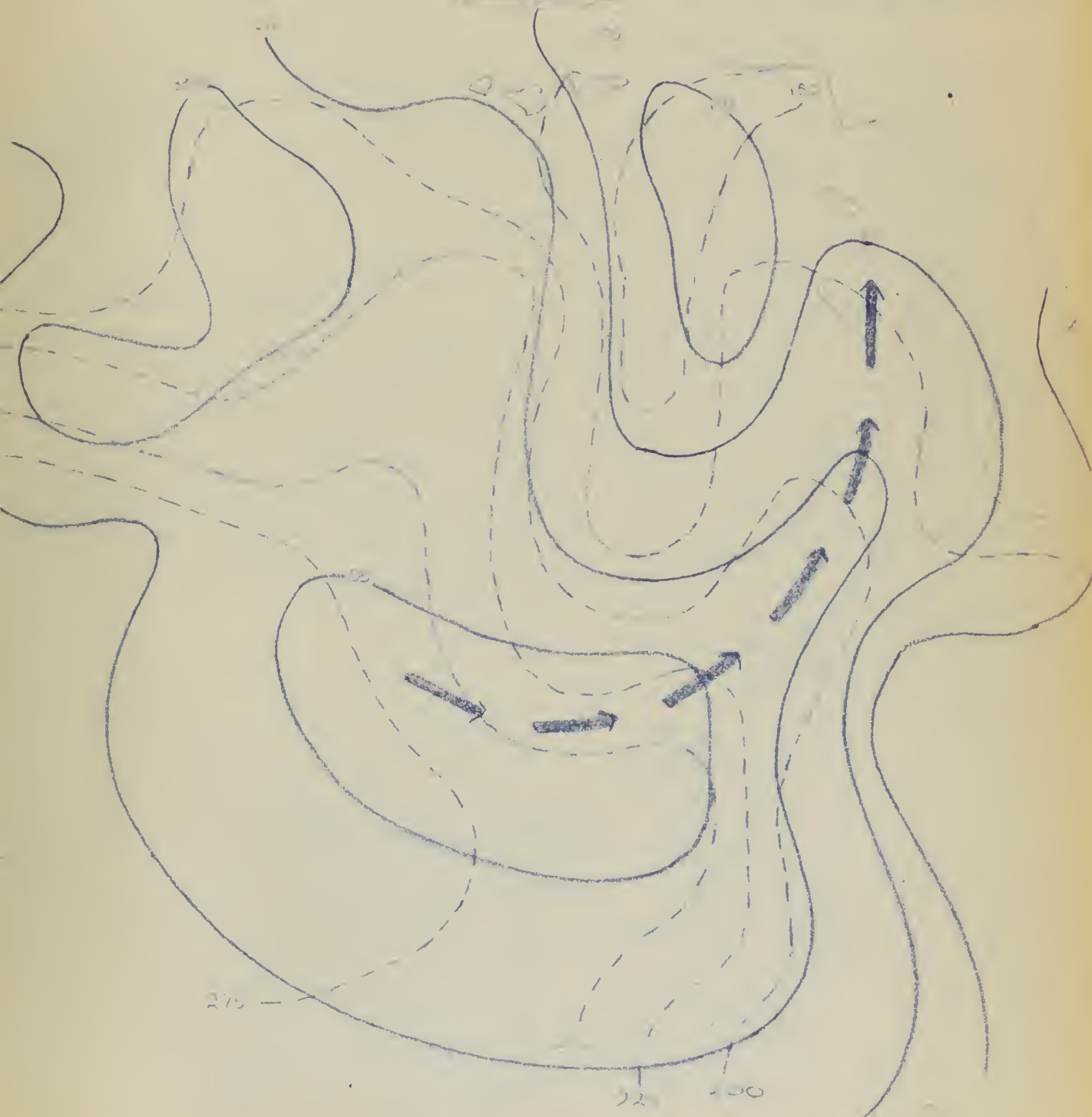




PLATE IX

Salinity distribution  
on  $\sigma_t = 26.00$  surface  
May 1950

- - - 25 meter isobaths

— Salinity in o/00  
(whole numbers 33 and 34  
omitted from isohaline  
labels)

➔ Inferred flow pattern

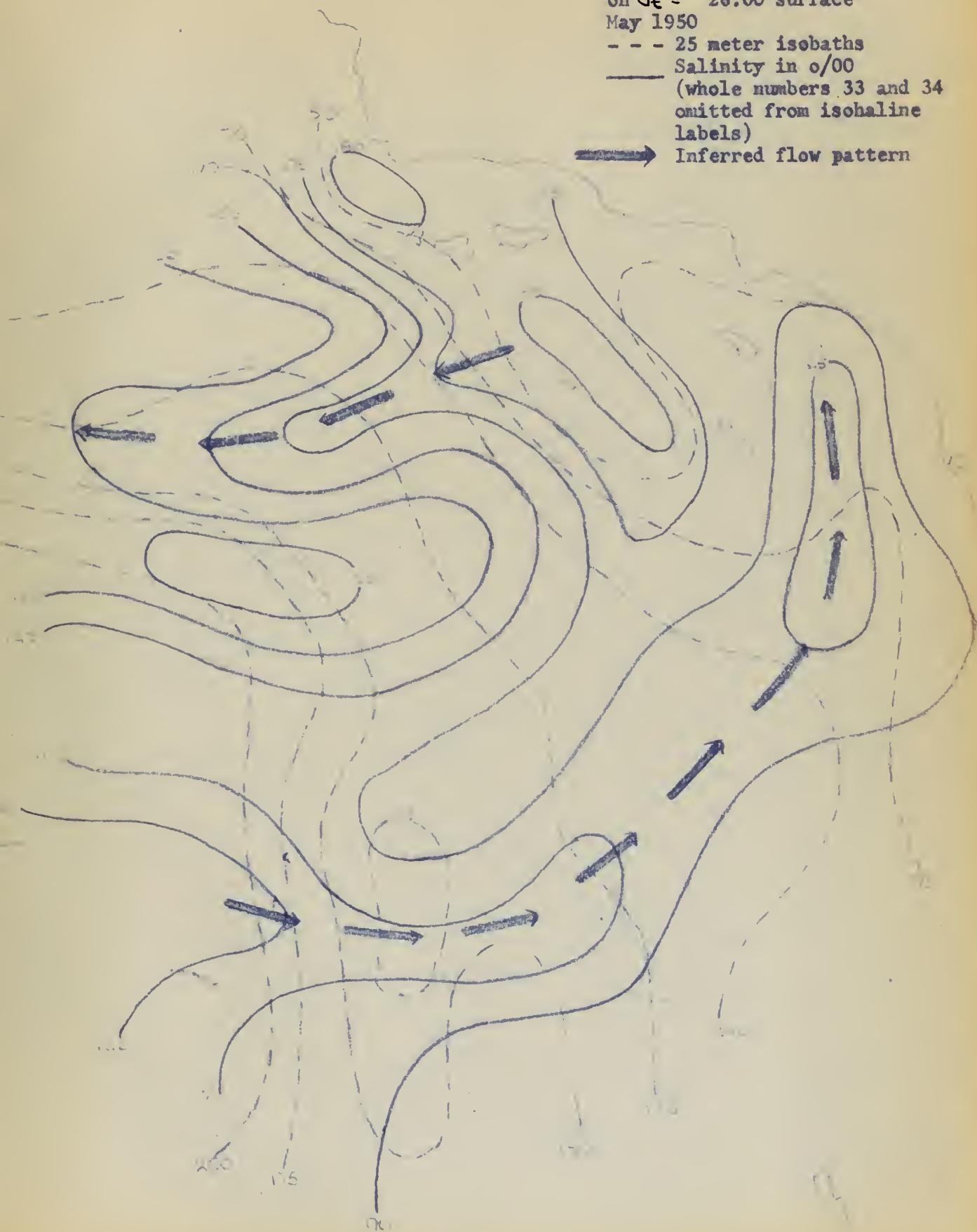





PLATE X

Salinity distribution  
on  $\sigma_t = 26.50$  surface  
May 1950

- - - 25 meter isobaths

—— Salinity in ‰  
(whole numbers 33 and 3  
omitted from isohaline  
labels)

 Inferred flow pattern

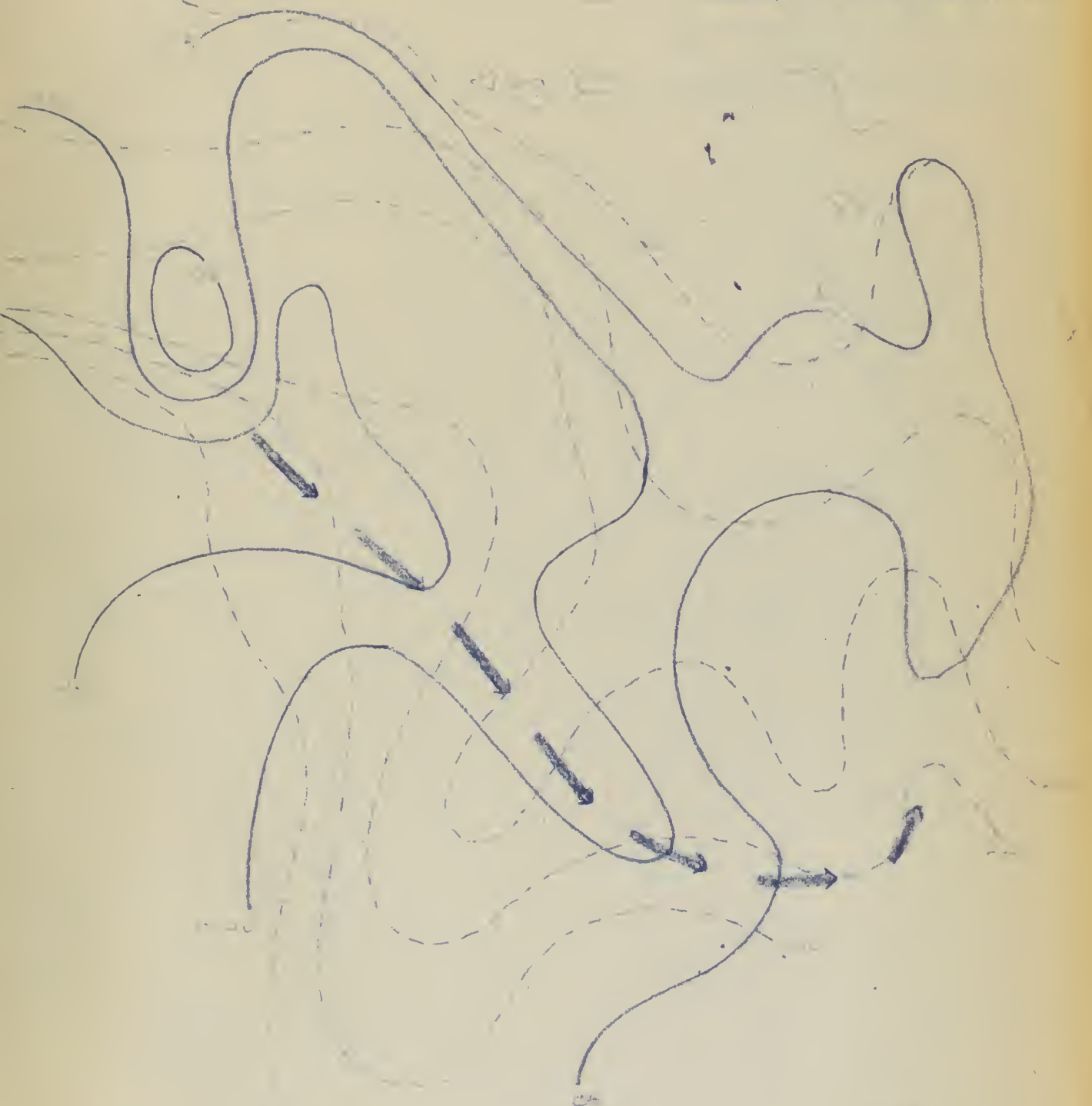






PLATE XI

Salinity distribution  
on  $\sigma_t = 26.00$  surface  
June 1950

- - - 25 meter isobaths  
—— Salinity in o/00  
(whole numbers 33 and 34  
omitted from isohaline  
labels)

➡ Inferred flow pattern

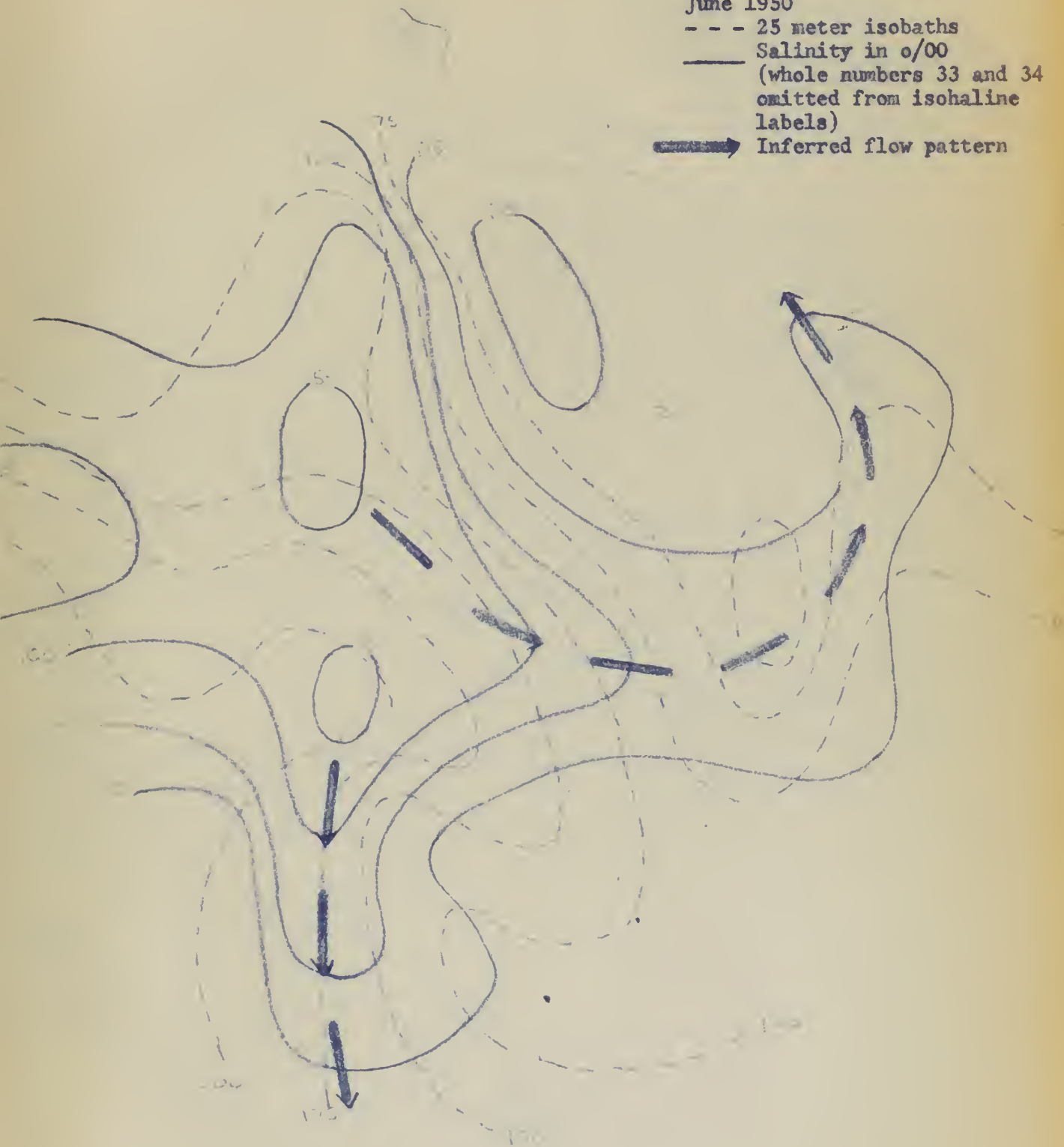




PLATE XII

Salinity distribution  
on  $\sigma_t = 26.50$  surface  
June 1950

- - - 25 meter isobaths

— Salinity in ‰  
(whole numbers 33 and 34  
omitted from isohaline  
labels)

➔ Inferred flow pattern

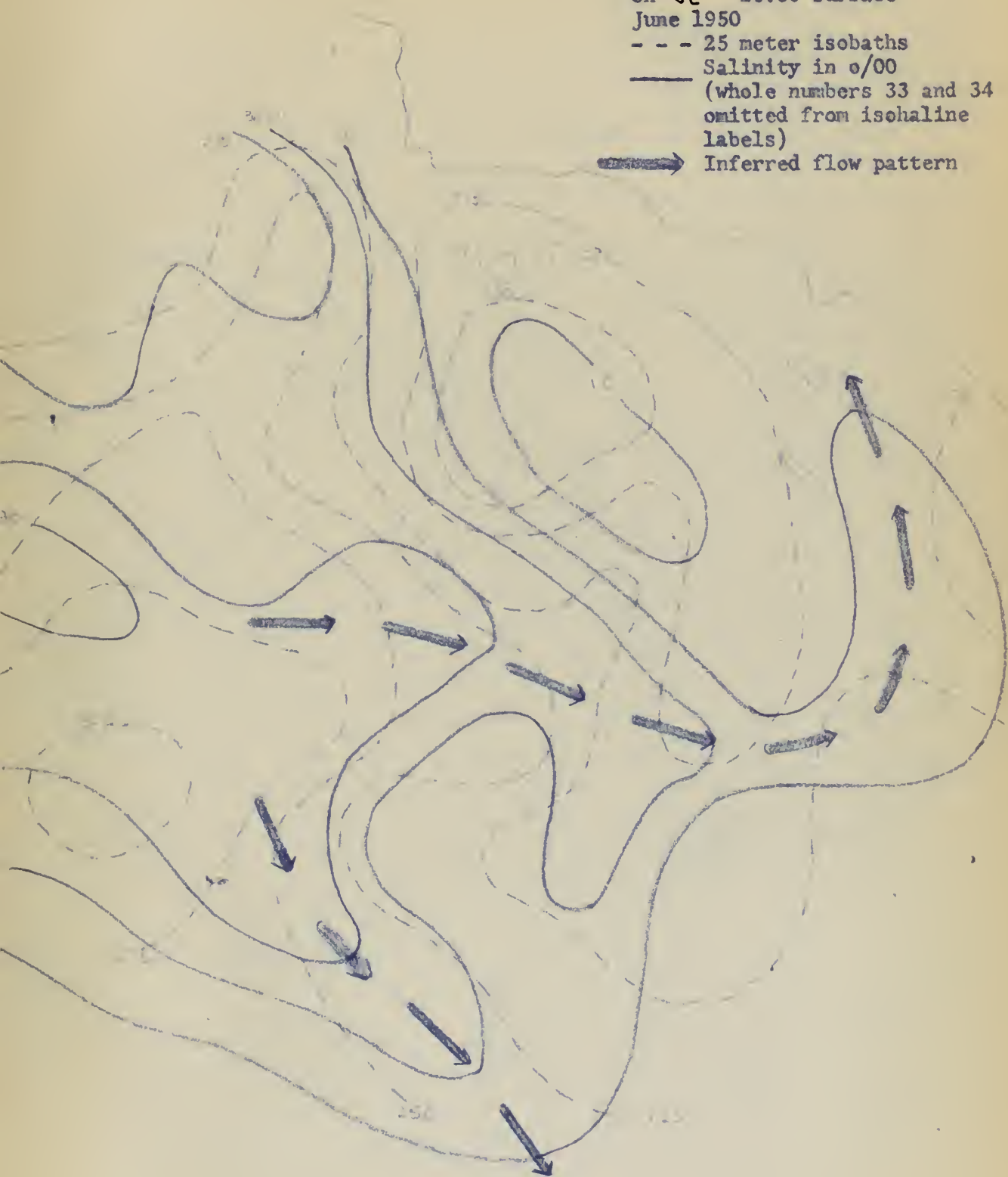




PLATE XIII

Salinity distribution  
on  $\sigma_t = 26.00$  surface  
July 1950

- - - 25 meter isobaths

— Salinity in o/00  
(whole numbers 33 and 34  
omitted from isohaline  
labels)

➔ Inferred flow pattern





Salinity distribution  
on  $\sigma_t = 26.50$  surface  
July 1950

- - - 25 meter isobaths
- Salinity in ‰ (whole numbers 33 and 34 omitted from isohaline labels)
- ➔ Inferred flow pattern

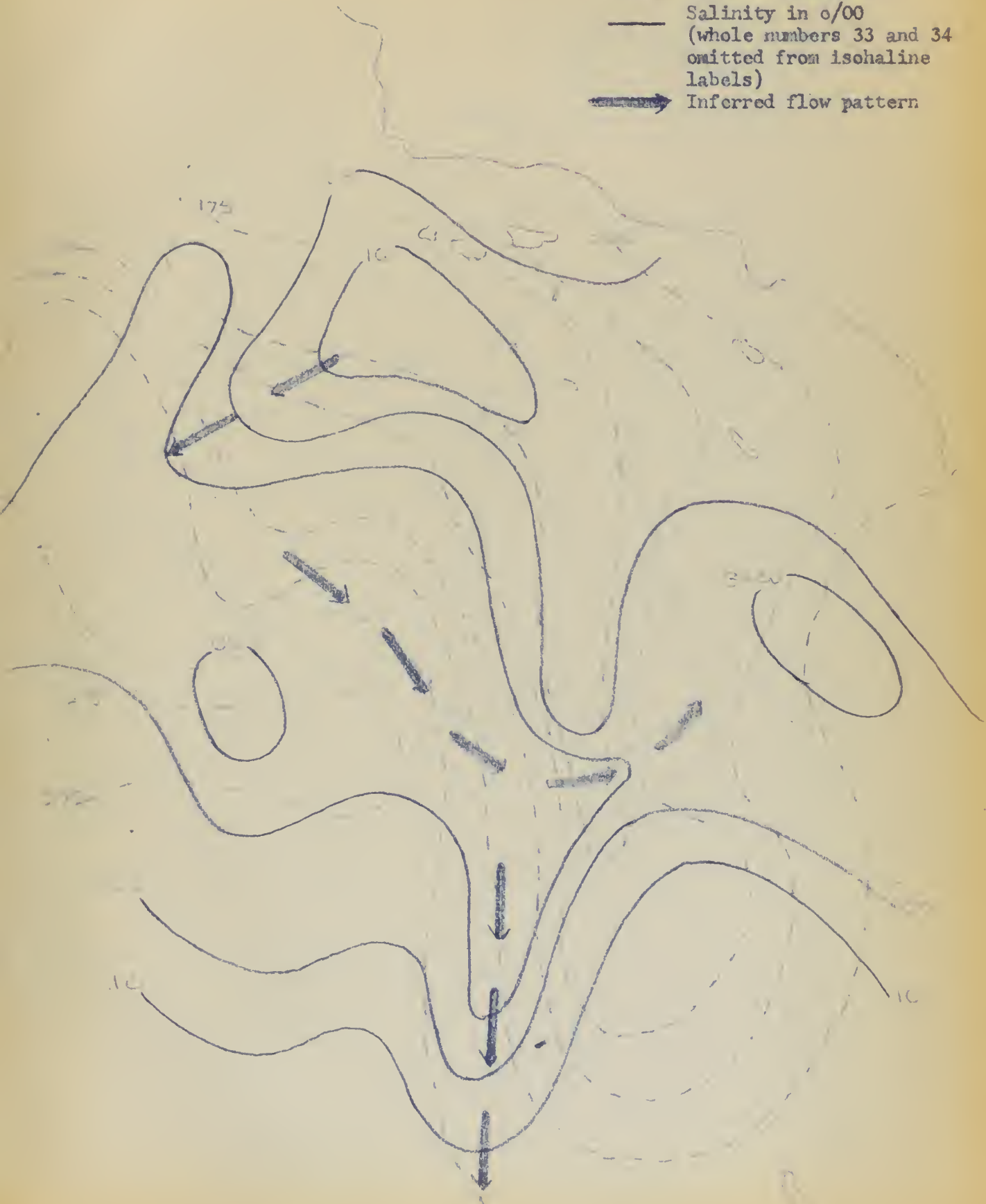






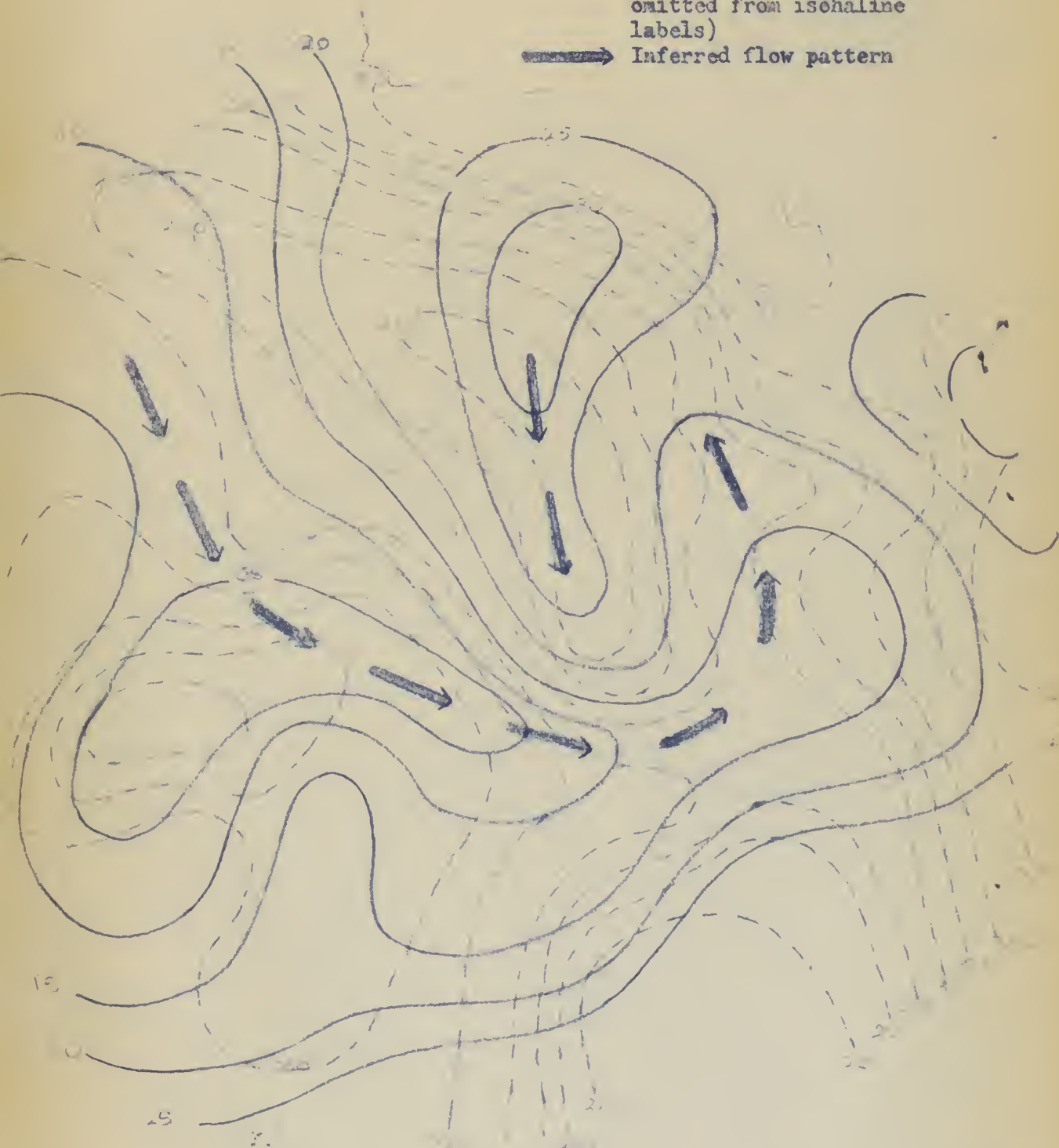
PLATE XV

Salinity distribution  
on  $\sigma_t = 26.75$  surface  
July 1950

- - - 25 meter isobaths

— Salinity in o/00  
(whole numbers 33 and 34  
omitted from isohaline  
labels)

➡ Inferred flow pattern





Salinity distribution  
on  $\sigma_t = 27.00$  surface  
July 1950

- - - 25 meter isobaths
- Salinity in ‰ (whole numbers 33 and 34 omitted from isohaline labels)
- ➡ Inferred flow pattern

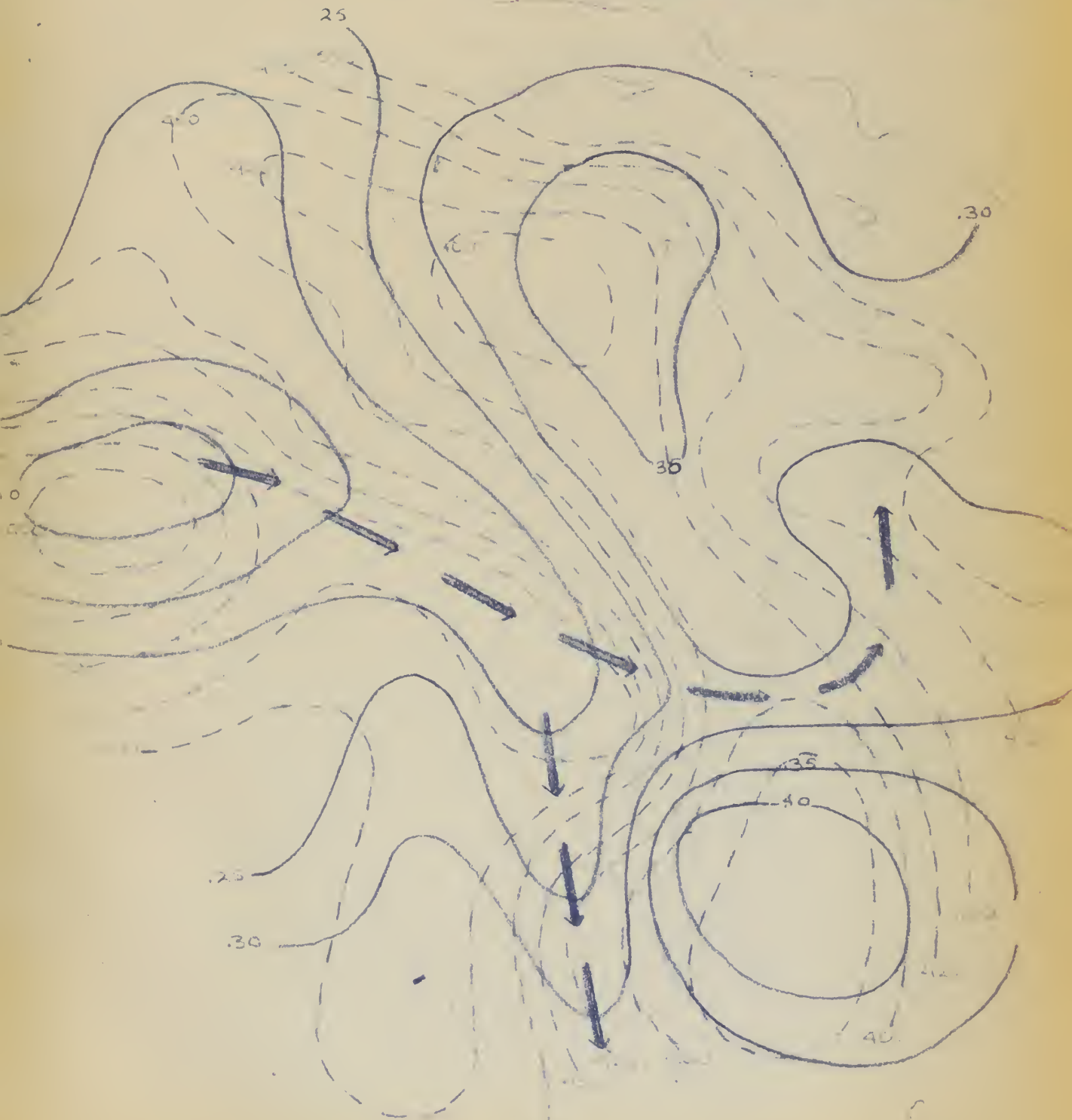




PLATE XVII

Salinity distribution  
on  $\sigma_t = 27.25$  surface  
July 1950

- - - 25 meter isobaths

— Salinity in ‰  
(whole numbers 33 and 34  
omitted from isohaline  
labels)

→ Inferred flow pattern















APR 19  
JUL 15  
JA 15  
FE 262  
FE 262  
FE 262

BINDERY  
765  
INTERLIB  
11402  
11402  
11402

19344

Thesis Seay  
S406 Use of isentropic analysis in deducing oceanic flow patterns in a region of upwelling.

★  
JUL 15  
JA 15  
FE 262  
AG 2664  
AG 2664  
17 JUN 65

BINDERY  
765  
INTERLIB  
11402  
114391  
14391  
14190

Thesis  
S406

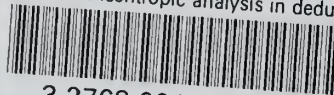
19344

Thesis Seay  
S406 Use of isentropic analysis in deducing oceanic flow patterns in a region of upwelling.

Library  
U. S. Naval Postgraduate School  
Monterey, California

thesS406

The use of isentropic analysis in deduci



3 2768 001 94442 4

DUDLEY KNOX LIBRARY